Real-time Detection of Infrared Radiation by Position-sensitive Superconducting Bolometer

Francesco Laviano, Roberto Gerbaldo, Gianluca Ghigo, Laura Gozzelino, Enrica Mezzetti
dept. Physics
Politecnico di Torino and INFN Sezione Torino
Torino, Italy
Email: francesco.laviano, roberto.gerbaldo, gianluca.ghigo, laura.gozzelino, enrica.mezzetti@polito.it

Luca Mesin
dept. Electronics
Politecnico di Torino
Torino, Italy
Email: luca.mesin@polito.it

Alberto Rovelli
Istituto Nazionale Fisica Nucleare
Laboratori Nazionali del Sud
Catania, Italy
Email: rovelli@lns.infn.it

***Abstract*—Infrared sensors are fundamental building blocks of strategic applications such as atmospheric gas monitoring, thermal imaging and telecommunications. While single frequency applications can employ resonant devices that have high resolution and high sensitivity, broad-band infrared detection relies on bolometric sensors. In this paper, we present a high-temperature superconducting sensor whose structural and electrical properties are locally modified by heavy-ion irradiation, in order to obtain position-sensitive broad band infrared detection. The bolometer, biased with constant current, responds to infrared radiation (from near to far-infrared spectra), with a dissipative voltage signal that can be monitored in real-time with a standard voltmeter. The digitized signal is processed with artificial neural networks (ANN) in order to correct for thermal and electronic noise contributions. Once trained, the ANN can be applied to new detected data and process them in real-time. In this way, real-time, position-sensitive detection of broad-band infrared radiation is achieved.**

***Index Terms*—Real-time sampling, superconducting devices, superconducting films, THz detector, neural networks.**

I. INTRODUCTION

Detection of infrared radiation is a fundamental task for many strategic applications in biomedical, environment monitoring, space science and military fields [1]. Since the very beginning of the research in these fields [2], much attention was paid to the low-frequency part of the infrared spectrum, the far-infrared (FIR), because many molecular absorption spectra are centered in this frequency range. However, the FIR radiation slightly interacts with solid state devices and therefore development of high responsivity devices is still a crucial task for many applications. Resonant devices [3] have high sensitivity for selected frequency ranges and operate at room temperature, making them the best choice for single frequency applications. On the other hand, wide band bolometric detection is commonly achieved with bolometers operated at liquid Helium temperature or below [1], making them expensive solutions (both for what concerns cost of instrumentation and size), sometimes limiting the operation time due to the cryogenic requirements, e.g., in satellite application. After the discovery of high temperature superconductors (HTSC) [4], promising applications of HTSC bolometers were envisaged, because they can be used above the liquid nitrogen temperature. In particular, several solutions have been already proposed for HTSC $YBa_2Cu_3O_{7-x}$ (YBCO) based bolometers that have been demonstrated to respond to the infrared radiation [5]. Since responsivity is corresponding to the resistance versus temperature slope, the maximum responsivity is achieved at the mid-point of the transition to the superconducting state. Optimally doped YBCO bolometers, whose critical temperature (Tc) is around 90 K, display the highest responsivity [6]. For what concerns high speed operation, thermal modeling suggested that thin membranes or suitable substrates should be used. In order to obtain a high responsivity and position-sensitive YBCO bolometer with controlled Tc, we employed irradiation with micro-collimated high energy heavy ion (HEHI) beams. In this way, Tc can be finely tuned (reduced), while the resistance versus temperature slope is totally preserved. Another chief result of this process is to confine the sensitive area to the irradiated part, therefore a position-sensitive detector is obtained. Detection of broad-band infrared radiation can be performed with standard four probe techniques used for resistance measurement, therefore real-time monitoring of infrared signals is achieved. Since the device is sensitive to the full infrared spectrum, thermal fluctuation is an important noise source along with Johnson noise. In order to correct for these major noise sources, we applied an artificial neural network (ANN) signal processing. The ANN processing eliminates the thermal background fluctuation and renormalizes the signal intensity due to the change in responsivity. In this way, real-time monitoring of infrared signals is achieved with a position sensitive detector that can be housed in a light weight, liquid nitrogen temperature dewar.

Copyright (c) IARIA, 2011. ISBN: 978-1-61208-145-8

II. METHODS

A. Device design and construction

YBCO films are deposited by thermal co-evaporation on MgO substrates [7]. YBCO film thickness is 250 nm, in order to obtain high critical current density, Jc, in the as-grown material [8]. Tc of as-grown samples is about 89 K, at the transition onset, and the transition width, ΔTc, is less than one kelvin. Sample patterning is obtained by standard UV photolithography and wet-etching in HCl/H_2O solution. The device layout consists of two meander structures, which are connected in series. One of them is uniformly irradiated with a suitable ion fluence, in order to obtain localized dissipation. The other meander serves as control signal for the background temperature monitoring [9]. The irradiation was performed at INFN laboratories [10], employing 114 MeV ^{197}Au ions for the controlled reduction of YBCO Tc. With a fluence of 4.84 $\cdot$ 10^{11} cm^{-2}, the zero resistance temperature is lowered by about 5 K.

B. Photoresponse measurements

Broad-band, continuous-wave infrared radiation is produced by a high pressure Hg arc lamp (OSRAM HBO 100W) [2]. The wavelength range is selected by proper filtering. In particular, high-resistivity n-type Si (flat transmittance above 50%), enables the transmission of the mid and far infrared (MIR-FIR) spectra (wavelength range 1-100 μm). The electrical measurements were performed by 4-probe method for each meander following the scheme reported in Figure 1 . The contacts were made by direct soldering Au wires (diameter of 50 μm for voltage pads and 125μm for current leads), on the YBCO pads with a low-temperature alloy (In-Sn-Bi). The electrical current was kept constant during the measurement (current source Keithley model 224) and the voltage signals were recorded in real-time (integration time 100 ms) by a dual channel nano-voltmeter (Keithley model 2182A). A custom Labview software was used for controlling the instruments (through GPIB interface) and for collecting the raw data on a PC.

C. Features selection and neural model

The output of the sensor is affected by thermal and electronic noise. In particular, thermal noise induces a nonlinear bias which increases as the sensor warms during the measurement. In order to compensate for the effect of noise, a nonlinear, real time signal processing technique was developed, based on ANN. ANNs are biologically inspired models consisting of a network of interconnections between neurons, which are the basic computational units. A single neuron processes multiple inputs and produces an output which is the result of the application of an activation function (usually nonlinear) to a linear combination of the inputs

$$y_i = \phi_i \left(\sum_{j=1}^{N} w_{ij} x_j + b_i \right) \qquad (1)$$

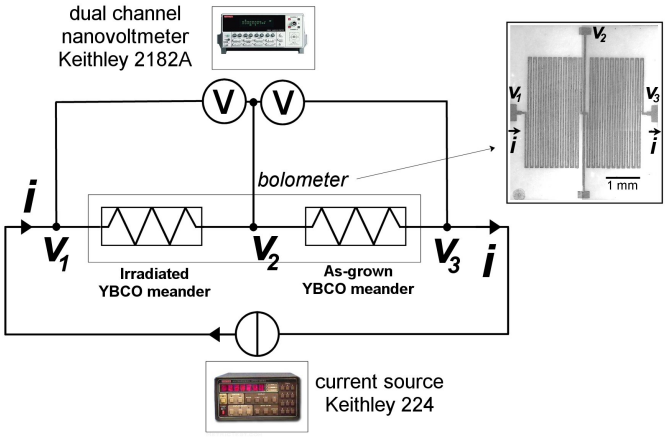

Fig. 1. Scheme of electrical measurement method. In the inset, a photo of the actual bolometer is shown.

where y_i is the output of the i^{th} neuron, ϕ_i is the activation function, w_{ij} is the weight between the j^{th} input x_j and the i^{th} neuron and b_i is a bias. The weights and the bias are free parameters that can be adaptively chosen in order to estimate an input-output map associating the input measurements to the desired output, provided by a set of training data.

The selection of optimal features that are going to be used as the input of the ANN is of great importance, in order to reduce the measurement and storage requirements, to counteract the difficulties of facing a problem with large dimension, to reduce noise content and to improve performance. We used a method based on the selection of the input data providing maximal information on the output. In order to avoid redundancy between input features, we used the algorithm proposed in [11] which determines the interdependencies between candidate variables computing the Partial Mutual Information (PMI). This technique found applications in feature selection for system identification in meteo forecast and in air pollution distribution prediction [12]. PMI represents the information between a considered variable and the output that is not contained in the already selected features. Variables with maximal PMI with the output are iteratively selected from the set of candidates.

The considered candidate variables were the values of the output of the sensor at the present instant and its delayed versions, with a time delay up to 5 samples. The desired output was the power of the source. Using PMI selection method, the candidate variables were ordered, starting from the one with maximum mutual information with the output and continuing with the input features in decreasing order of PMI with the output. Then, to map the input to the desired output, a set of multilayer perceptrons (MLP) was used. Different MLPs were obtained using a different number of inputs, a single hidden layer with number of neurons in the range $1 - 10$ (with sigmoidal activation function) and a single output neuron (with linear activation function). Different MLP topologies were trained by modifying iteratively the weights and the bias in order to reduce the error in fitting the desired output, using

Copyright (c) IARIA, 2011. ISBN: 978-1-61208-145-8

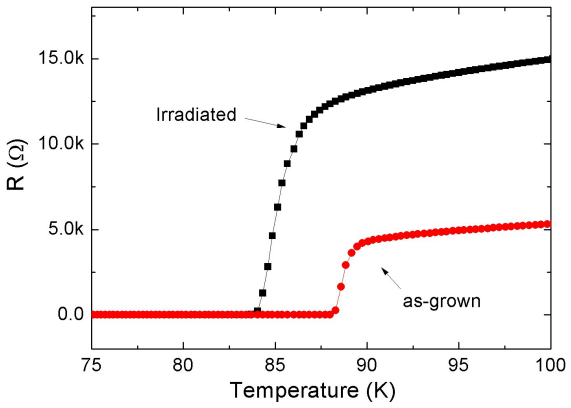

Fig. 2. Resistance versus temperature behavior of irradiated and as-grown YBCO (bias current 10 μA). The Tc difference is around 5 K (114 MeV ^{197}Au 4.84 $\cdot$ 10^{11} ion cm^{-2}). Note that the resistance versus temperature slope is preserved.

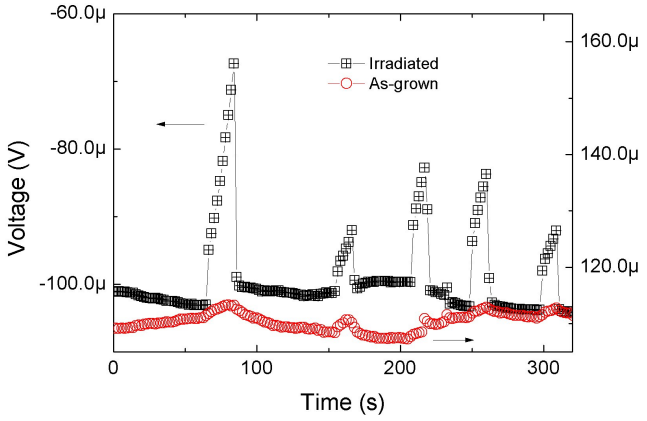

Fig. 3. Sample signals of both irradiated and as-grown meanders. The infrared beam is coming from a black-body source which is turned on and off by means of an electro-mechanical shutter. The irradiated meander responds with sharp jumps to the infrared beam, while the as-grown meander displays a signal whose evolution is determined by the background temperature.

the quasi-Newton algorithm with a number of iterations in the range $10 - 50$.

Data included 5 radiation events with constant power. Each ANN was trained with a portion of signal including 4 of the 5 events and tested on a portion of signal including the remaining one (test set). All root mean squared (RMS) errors on the test data were computed and the ANN with minimum average error across the 5 trials was selected as that with best generalization performance.

III. Results

The resistance versus temperature characteristics of the device are shown in Figure 2. The irradiated meander displays increased resistivity and lowered Tc with respect to the as-grown structure, as expected. The working point for the device is around the onset of dissipation of the irradiated meander (around T = 81.5 K with a bias current of 1 mA [9]).

If the device is exposed to infrared radiation, the local temperature will raise and only the irradiated meander displays dissipative signals, as shown in Figure 3.

The voltage picked up on the as-grown meander is due to the thermoelectric signal spreading from the irradiated YBCO and therefore it is indicating the variation of the substrate temperature. On the other hand, the temperature fluctuations due to the infrared radiation to be detected and to the environment are changing the responsivity of the bolometer: the voltage is continuously increasing when the infrared beam hits the detector. In order to correct for these problems due to the thermal backgroung, we applied an ANN signal processing as described above. For each of the five training experiments, PMI selected the present measurement as the feature with maximal mutual information with the radiated power and the one step delayed measure as the feature with maximal partial mutual information with the desired output, once selected the present measure. The selected optimal ANN, with best

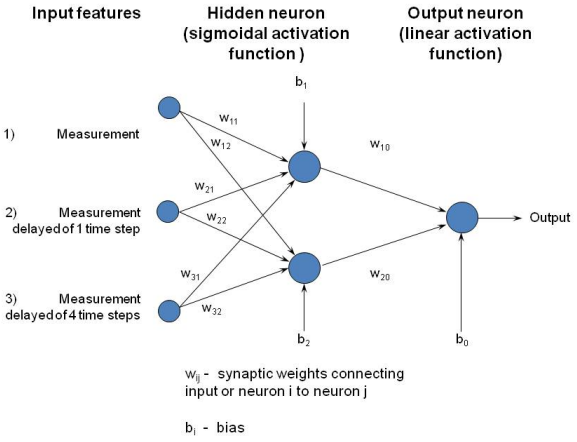

Fig. 4. Topology of the ANN with best generalization performances.

generalization to the test set (average generalization error about 2.5%), has three inputs and two hidden neurons (see Figure 4) and was trained for 30 iterations. Figure 5 shows the raw data and the infrared radiation estimated by the optimal ANN for one choice of the training and the test sets. Good performances (average generalization error about 10%) were obtained also using two input features (the present measure and the 1 step delayed measure) and a single hidden neuron.

IV. Conclusion

We have tested a high-temperature superconducting bolometer for monitoring infrared signals in real-time. High responsivity is obtained for temperature just above the liquid nitrogen temperature thanks to the local irradiation with HEHI which reduces in a controlled way the critical temperature but retains the resistance versus temperature slope. Since the

Copyright (c) IARIA, 2011. ISBN: 978-1-61208-145-8

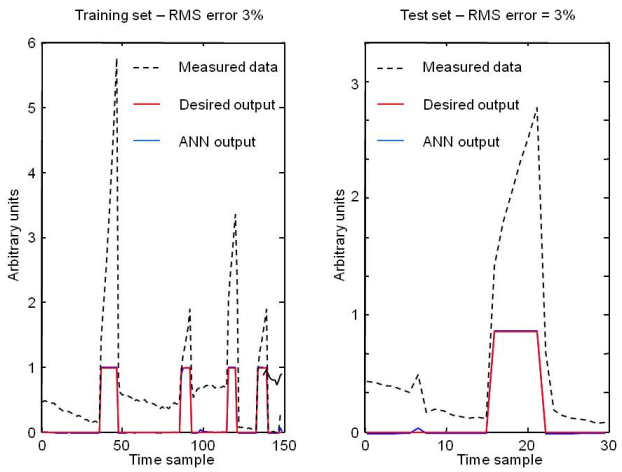

Fig. 5. Raw data, desired output and ANN estimated output for an example of training set and test set.

infrared radiation to be detected is coupled with a noisy thermal background, we implemented an ANN approach in order to obtain the subtraction of the thermal background and the renormalization of the output intensity in dependence on such background. Once trained and validated on experimental signals, the ANN can filter new detected data in real-time.

Different MLPs were tested. Optimal performances were achieved using MLPs with simple topology. Good performances were obtained using only the actual measure and the 1 step delayed one. This selection of inputs indicates that the measurement and its time derivative are sufficient to estimate the required output. In that case, only one neuron in the hidden layer was required. This is due to the binary desired output. The optimal MLPs was a bit more complicated, as a further delayed version of the measure was selected and one more neuron was placed in the hidden layer. This choice improved the stability of the estimates to noise, improving slightly the performances. It is worth noticing that to detect the presence of a constant radiation, the output neuron could also have a sigmoidal activation function. Future investigation will be devoted to the estimation of an arbitrary profile of thermal radiation. In such a case, a linear activation function for the output neuron is preferred. Moreover, a more complex topology of the network is expected to be able to optimally adapt to the data.

This study demonstrates the possibility to develop high responsivity infrared bolometers based on superconducting oxides which are working at temperature above the liquid nitrogen. The suitably engineered detector in a portable, light-weight cryostat is desired for molecular spectroscopy, thermal imaging and telecommunications.

V. Acknowledgment

This work was partially supported by INFN-MONADE and INFN-TERASPARC projects and by the national project AWIS (Airport Winter Information System), funded by Piedmont Authority, Italy.

References

[1] P. H. Siegel, *Terahertz Technology,* IEEE Trans. on Microwave Theory and Techniques, vol. 50, no. 3, pp. 910-928, 2002.

[2] M.F. Kimmitt, *Restrahlen to T-Rays - 100 Years of Terahertz Radiation,* Journal of Biological Physics, vol. 29, pp. 77-85, 2003.

[3] W. Knap, F. Teppe, Y. Meziani, N. Dyakonova, J. Lusakowski, F. Boeuf, T. Skotnicki, D. Maude, S. Rumyantsev and M. S. Shur, *Plasma wave detection of sub-terahertz and terahertz radiation by silicon field-effect transistors,* Appl. Phys. Lett. vol. 85, pp. 675-677, 2004.

[4] J. G. Bednorz and K. A. Mller, *Possible high Tc superconductivity in the Ba-La-Cu-O system,* Zeitschrift fr Physik B Condensed Matter 64, pp. 189-193, 1986.

[5] A.J. Kreisler and A. Gaugue, *Recent progress in high-temperature superconductor bolometric detectors: from the mid-infrared to the far-infrared (THz) range,* Supercond. Sci. Technol. 13 pp. 1235-1245, 2000

[6] A. Jukna and R. Sobolewski, *Time-resolved photoresponse in the resistive flux-flow state in YBaCuO superconducting microbridges,* Supercond. Sci. Technol., vol. 16 pp. 911-915, July 2003

[7] B. Utz, R. Semerad, M. Bauer, W. Prusseit, P. Berberich, and H. Kinder, *Deposition of YBCO and NBCO films on areas of 9 inches in diameter,* IEEE Trans. Appl. Supercond., vol. 7, no. 2, pp. 1272-1277, 1997.

[8] F. Laviano, D. Botta, R. Gerbaldo, G. Ghigo, L. Gozzelino, L. Gianni, S. Zannella, and E. Mezzetti, *Thickness dependance of the current density distribution in superconducting films,* Physica C, vol. 404, pp. 220-225, 2004.

[9] F. Laviano, R. Gerbaldo, G. Ghigo , L. Gozzelino, B. Minetti, A. Rovelli, and E. Mezzetti, *THz detection above 77K in YBCO films patterned by heavy-ion lithography,* IEEE Sensors Journal, vol. 10, pp. 863-868, 2010.

[10] A. Rovelli, A. Amato, D. Botta, A. Chiodoni, R. Gerbaldo, G. Ghigo, L. Gozzelino, F. Laviano, B. Minetti, and E. Mezzetti, *A new apparatus for deep patterning of beam sensitive target by means of high energy ion beam,* Nucl. Instrum. Methods Phys. Res. B, vol. 240, no. 4, pp. 842-849, 2005.

[11] A. Sharma, *Seasonal to interannual rainfall probabilistic forecasts for improved water supply management: 1 - A strategy for system predictor identification,* Journal of Hydrology, vol. 239, pp. 232-239, 2000.

[12] L. Mesin, F. Orione, R. Taormina, E. Pasero, *A feature selection method for air quality forecasting,* Proceedings of the 20th International Conference on Artificial Neural Networks (ICANN), Thessaloniki, Greece, September 15-18, 2010.

Copyright (c) IARIA, 2011. ISBN: 978-1-61208-145-8